


Preparation of flexible bone tissue scaffold utilizing sea urchin test and collagen

Naga Vijaya Lakshmi Manchinasetty^{1,2} · Sho Oshima^{2,3} · Masanori Kikuchi^{1,2} 

Received: 22 June 2017 / Accepted: 21 September 2017 / Published online: 13 October 2017
© Springer Science+Business Media, LLC 2017

Abstract Gonads of sea urchin are consumed in Japan and some countries as food and most parts including its tests are discarded as marine wastes. Therefore, utilization of them as functional materials would reduce the waste as well as encourage Japanese fishery. In this study, magnesium containing calcite granules collected from sea urchin tests were hydrothermally phosphatized and the obtained granules were identified as approximately 82% in mass of magnesium containing β -tricalcium phosphate and 18% in mass of nonstoichiometric hydroxyapatite, *i.e.*, a biphasic calcium phosphate, maintaining the original porous network. Shape-controlled scaffolds were fabricated with the obtained biphasic calcium phosphate granules and collagen. The scaffolds showed good open porosity (83.84%) and adequate mechanical properties for handling during cell culture and subsequent operations. The MG-63 cells showed higher proliferation and osteogenic differentiation in comparison to a control material, the collagen sponge with the same size. Furthermore, cell viability assay proved that the scaffolds were not cytotoxic. These results suggest that scaffold prepared using sea urchin test derived calcium phosphate and collagen could be a potential candidate of

bone void fillers for non-load bearing defects in bone reconstruction as well as scaffolds for bone tissue engineering.

1 Introduction

The prevalence of bone disorders and conditions has increased steeply and are expected to increase especially in aging populations, due to rapid obesity and poor physical activity. Further, gait disorders, one of their causes is pedal skeletal tissue disorder, is considered to relate with senile dementia. Bone is a dynamic, highly vascularized tissue with a unique capacity to heal by bone remodelling process if the surrounding circumstances are suited for remodelling. The major role of bone is a physical one, withstands load bearing and protects the internal organs of the body. Hence, major alterations in bone's structure due to injury or disease can dramatically alter one's body equilibrium and quality of life [1, 2]. Current clinical treatments for bone repair and regeneration include autografts and allografts. To date, autografts serve as the gold standard because they are histocompatible and non-immunogenic but they have several disadvantages like donor site morbidity, deformity, scarring and chronic pain. The second choice is allograft involving bone transplantation from a cadaver. However, allografts are associated with risk of immunoreactions and transmission of infections [3, 4].

The field of bone tissue engineering (BTE) was introduced three decades ago and focuses on alternate treatment options that will ideally eliminate previously described issues of current clinical treatments. The BTE aims to induce new functional bone regeneration via the synergistic

✉ Masanori Kikuchi
KIKUCHI.Masanori@nims.go.jp

¹ Division of Bioengineering and Bioinformatics, Graduate School of Information Science and Technology, Hokkaido University Kita-14, Nishi-9, Kita-Ku, Sapporo, Hokkaido 060-0814, Japan

² Bioceramics Group, Research Center for Functional Materials, National Institute for Materials Science, 1-1 Namiki, Tsukuba, Ibaraki 305-0044, Japan

³ Design and Production Process Engineering, Graduate School of Science and Engineering, Ibaraki University, Ibaraki, 4-12-1, Nakanarusawa, Hitachi 316-8511, Japan

combination therapy of biomaterials, cells and biochemical factors [5, 6]. Bone is a heterogeneous composite material, consisting of a mineral component mainly hydroxyapatite, an organic component mainly collagen and water. Several approaches have been made in the field of BTE to mimic the bone composition and structure. Essential properties of a scaffold are biocompatibility, porosity, pore interconnectivity, osteoconductivity, osteoinductivity, adequate mechanical strength, and biodegradability [7, 8]. A three-dimensional interconnection (3D) of both macropores ($>100\ \mu\text{m}$) and micropores ($<50\ \mu\text{m}$) are important for a porous scaffold because macropores allow cell and tissue invasion and micropores allow efficient exchange of nutrients and wastes [9]. Ceramics [10], synthetic and natural polymers [11] were studied and used for the fabrication of BTE scaffolds. Among ceramics, hydroxyapatite (HAp) and β -tricalcium phosphate (β -TCP) porous ceramics have been widely studied and used as bone substitutes due to their biocompatibility, osteoconductivity and close resemblance to original bone composition [12, 13].

Recently, marine-derived biomaterials from corals [14, 15], sponges [16], cuttlebone [17], and sea urchins spines [18] have shown good potential as bone substitutes. Marine organisms provide a natural reservoir of porous structures with a wide range; the minerals found in them are generally calcium carbonate in the form of aragonite or calcite and can be easily converted to calcium phosphates by hydrothermal conversion [19]. Marine organisms are also a rich source of ions like carbonate (CO_3^{2-}), magnesium (Mg^{2+}) and silicate (SiO_4^{4-}) which can be incorporated into a biomaterial when converting the base mineral to calcium phosphate. Magnesium has been reported to enhance osteoblast adhesion, angiogenesis in porous structures [20] and increase bioresorption [21], carbonate and silicon substituted calcium phosphates have been shown to enhance the bone formation in vivo [22, 23]. So, just by simply choosing the biogenic source of calcite or aragonite, a range of ion substitutions is possible, obtained by simple process compared to the some complex processes required to produce ion-substituted ceramics [24]. Work on the use of marine organisms as a bone substitute resulted in commercialization of two well-known products namely, Pro-osteonTM and Biocoral[®], derived from stony corals. Although these products have been available for many years, their use in the clinic remains low due to their poor bioresorption [25, 26].

Also, corals are considered as a reservoir of carbonate gas to decrease greenhouse effect as well as a key organism to maintain marine ecosystem as a coral reef; thus their collection from the sea is strongly restricted worldwide [27]. Whereas, sea urchins are widely consumed as food in Japan and some countries and their shells (tests) are discarded as wastes of food processing. The total amount of sea urchin

food processing waste in Hokkaido area of Japan was estimated to be approximately 4000 metric tons in 2013 [28]. The costs of disposal are mainly borne by the fisherman, thus utilization of sea urchin tests would reduce the waste as well as encourage Japanese fishery.

Conversions of sea urchins shell to calcium phosphate powders were reported [29, 30]; however, preservation of their unique microstructure after the conversion process and evaluation of their biocompatibility had not been reported yet. The skeleton of sea urchin consists of porous interconnected network (stereom) with both macro and micropores, and its porosity was reported to be more than 50% in volume [31]. They seem suitable for fabrication of 3D scaffold if the test granules are bound with the help of biocompatible polymers, such as collagen, gelatin or other synthetic polymers. This paper describes the preparation of porous biphasic calcium phosphate granules from sea urchin tests by hydrothermal phosphatization and subsequent preparation and evaluation of the scaffold fabricated with the biphasic calcium phosphate granules and collagen.

2 Materials and methods

2.1 Materials

Chemicals used in this research were purchased from Wako Pure Chemical Ltd., Japan if that without further notice. Tests of sea urchins, *strongylocentrotus nudus* and *strongylocentrotus intermedius* were kindly provided from the Shakotan-cho, Hokkaido prefecture, Japan. Skeletons of the sea urchin tests were obtained by removal of their organic substances by soaking in commercial bleach solution (Kitchen power bleach, Lion Hygiene Corporation) at 10% in volume, several-time washing with distilled water, soaked in warm water overnight to remove excess chlorine, washed with distilled water again and dried in an oven at 60 °C. The skeleton obtained from *strongylocentrotus intermedius* is denoted as SU1 and that from *strongylocentrotus nudus* is denoted as SU2.

2.2 Hydrothermal phosphatization

The skeletons, SU1 or SU2, were crushed by hand and hydrothermally treated in Teflon[®] lined stainless steel autoclave (300 mL of internal volume, Taiatsu Techno[®] Corporation) at 180 °C for 6 days with 200 mL of 750 mM $(\text{NH}_4)_2\text{PO}_4$ and 25 mL of 300 mM KH_2PO_4 i.e., filling ratio of 75 % in volume. After 6 days of treatment, the autoclave was quenched with tap water. The solid phase was collected by filtration, cleaned in distilled water by an ultrasonication (Ultrasonic multi cleaner, W-113, Honda, Japan) for 5 min

and dried in an oven overnight at 60 °C. The skeletons phosphatized from SU1 and SU2 are denoted as CP1 and CP2, respectively.

2.3 Characterization of sea urchin skeletons

Microstructures and pore morphologies of them were observed by the scanning electron microscopy (SEM, S4800, Hitachi, Japan) with a Pt coating. The diameter of macropores and micropores were calculated according the method mentioned in ISO 13175-3. Qualitative chemical analyses of them were qualitatively identified by the energy dispersive X-ray spectroscopy (EDS, E-maxEvolution, Horiba Ltd., Japan) equipped with the SEM.

The CP1 and CP2 were calcined to be the respective CPC1 and CPC2 at 1000 °C for 30 min with a furnace (Nabertherm®, N150/14, Lillenthal, Germany) to examine the stability of crystal phases. Crystal phases of the SUs, CPs and CPCs were identified by the powder X-ray diffractometry (XRD, RINT-Ultima III, Rigaku Corporation, Japan) using $\text{CuK}\alpha$ from 10 to 60° for 2θ at a scanning rate of 2°/min. Ratios of calcium phosphate phases formed in the CP1 and CP2 was calculated from one selected XRD peak of calcium phosphate phases using a standard curve. The standard curve was calculated using the same peaks from XRD patterns of serial mixtures of pure calcium phosphates, contained in the obtained CPs. The Ca/P atomic ratio was calculated by using relative intensity of 3 0 0 diffraction line of HAp (32.90°) and 0 2 10 diffraction line of TCP (31.03°).

Transmission infrared spectra of the SUs, CPs and CPCs were measured by the KBr (Sigma Aldrich, USA) pellet method with a Fourier-transformed infrared spectrometer (FT-IR, Nicolet 4700, Thermo Electron Corporation, Japan).

Quantities of calcium, magnesium and phosphorus for SUs, CPs and CPCs were measured by the inductively coupled plasma atomic emission spectroscopy (ICP-AES, SPS7800, SII, NanoTechnology, Japan). The samples of 50 mg were dissolved in 5 mL of aqueous solution of HNO_3 1% in mass, and the sample solutions were subsequently diluted at 1:200 with the same HNO_3 solution for the ICP-AES analysis.

The results of characterization mentioned above were almost the same except for the ICP-AES and quantitative XRD analyses; hence, the CP2 and CPC2 results on physicochemical analyses are mainly used for further discussion in this paper.

2.4 Fabrication of scaffolds

The CP1 or CP2 was crushed and classified into granules of 1–2 mm in size by the sieving. Collagen solution of 1% in

mass was prepared by dissolving freeze-dried porcine dermal type-I atelocollagen (Nitta Gelatin, Japan) sponges in 0.1 M acetic acid solution (pH 3.0). Prior to fabrication, the collagen solution was neutralized with 1 N NaOH and adjusted its ionic strength to the physiological condition with 10× phosphate buffered saline (PBS, Sigma Aldrich, USA). Scaffolds were fabricated by mixing the granules with the collagen solution at a ratio of 1:2 (mass/volume), transferred into an acrylic mold with 10 mm in inner diameter and 15 mm in height and kept in an incubator at 37 °C for 2 h for collagen gelation. After the gelation, the mold was transferred to a –20 °C freezer for 24 h and freeze-dried (VirTis, Advantage, Maruto, Japan) at –20 °C overnight. The scaffolds were removed from the mold after freeze drying and dehydrothermally crosslinked at 140 °C for 12 h under vacuum (Eyela, VOS-2015D, Tokyo Rikakikai co., Ltd, Japan). The scaffold fabricated with the CP1 granules is denoted as CP1Col and that with the CP2 granules is denoted as CP2Col.

2.5 Characterization of scaffolds

The morphology of the horizontal cross section of the scaffolds was examined using the SEM. The open porosity of the scaffolds was measured by the liquid displacement method [32] using absolute ethanol as the displacement liquid to prevent the scaffolds from swelling or shrinking. Briefly, the scaffold was immersed in the absolute ethanol for 30 min. The scaffolds were weighed before (W_d), during (W_1) and after immersing (W_w). The porosity of the scaffolds was calculated using the formula (1) given below. The experiment was carried out in triplicates.

$$\text{Porosity}(\%) = \frac{W_w - W_d}{W_w - W_1} \times 100 \quad (1)$$

The stability of the scaffolds in physiological conditions was confirmed by a soaking in PBS at 37 °C for 7 days with a naked-eye observation.

The bending strengths of the scaffolds were measured with a universal testing machine equipped with a 1 kN load cell (AGS-H 1 kN, Shimadzu, Japan). The scaffolds were fabricated in the dimension of 40 mm in length, 8 mm in width and 6 mm in height. For wet condition analysis, the scaffolds were soaked in PBS at room temperature and 37 °C, 24 h prior to measurement. Each five specimens were measured at a crosshead speed of 0.5 mm/min, and three-point bending strength was calculated.

2.6 In vitro cell culture

The human osteoblast-like cell line, MG-63, derived from human osteosarcoma was used for the experiment. The MG-63 cells were subcultured in 75 cm² tissue culture flasks

using a complete medium, Dulbecco's modified Eagle's medium (DMEM, Sigma Aldrich, USA) supplemented with 10% (v/v) fetal bovine serum (Sigma Aldrich, USA) and 1% (v/v) penicillin/streptomycin (Gibco[®], Life technologies, Japan) in an incubator (HERAcell 150i, Thermo Scientific, Japan) at 95% relative humidity and 5% CO₂.

The CP1Col and CP2Col scaffolds were fabricated in the dimension of 10 mm in diameter and 5 mm in height. A collagen sponge as the same size as the scaffold was used as a control. All the scaffolds and sponges were sterilized by the ethylene oxide gas (EOG) method and conditioned with the complete medium at 37 °C for 3 h. After absorbing away the medium from the scaffolds using a sterilized filter paper (Advantec, 5C, 90 mm), the scaffolds were placed in a tissue culture dish (100 × 20 mm, FALCON[®] USA), 8 × 10⁵ cells suspended in 60 μL of the complete medium was seeded onto each scaffold and incubated at 37 °C for 2 h. After the incubation, the cell-seeded scaffolds were transferred into each well of 6-well plates (Gibco[®], USA). Then, 6 mL of the complete medium was added to each well and cultured for 7 days in the incubator. The medium was refreshed every 2 days.

After 7-day culture, osteoblastic differentiation was induced by an osteogenic medium, the complete medium supplemented with 10 mM β-glycerolphosphate (Reagent Grade, Sigma Aldrich, USA) and 50 μg/mL ascorbic acid. The osteogenic medium was refreshed every 2 days and cultured for 21 days. At various time intervals, the cell-scaffold constructs were harvested and used for the assays of cell adherence, DNA content, viability/cytotoxicity and osteoblast differentiation. The results of the CP1Col and CP2Col were the same for many assays; hence the results of the CP2Col are shown and discussed in this paper as the representative except for further notice.

2.7 Observation of cell adherence

The cell-scaffold constructs after 1- and 7-day culture were fixed with 10% neutral buffered formalin solution at room temperature for 2 days. After 2 days, the fixed constructs were removed, washed with distilled water thrice, dehydrated in graded series of ethanol and freeze-dried. The mid vertical cross section of the freeze-dried constructs was observed for cell adhesion and distribution using SEM.

2.8 Viability/cytotoxicity assay

Cell viability was evaluated by the live/dead cell staining assay using cell stain double staining kit (Dojindo Laboratories, Japan) according to the manufacturer's instruction. Briefly, the cell-scaffold constructs at 1- and 7-day cultures were washed thrice with PBS (Sigma Aldrich, USA) and incubated in 2 μM calcein-AM and 4 μM propidium iodide

solution in the PBS for 15 min. After the incubation, the constructs were observed for live and dead cells using a fluorescence microscope (BX51Olympus Corp., Japan) immediately.

2.9 DNA content

The cell proliferation in the scaffolds was quantified by the DNA amount in the cell-scaffold constructs. After 1-, 7-, 14- and 21-day cultures, each construct was harvested, homogenized on ice in the glycine lysis buffer containing 0.1 M glycine (pH 10.4), 1 mM MgCl₂ and 0.2% (v/v) TritonX-100 and incubated for 15 min in an ice box. Each sample was centrifuged at 12,000 rpm for 5 min, and the supernatant was transferred to a new centrifuge tube and stored at -80 °C until further analysis. The total DNA content was measured with a multiplate reader (GENius; TECAN, Männedorf, Switzerland) by the Hoechst 33258 method. Briefly, 100 μL of diluted sample was mixed with 100 μL of Hoechst dye 33258 (Dojindo Laboratories, Japan) in a 96-well microplate (FALCON[®], USA). Emissions at 458 nm excited by 360 nm light were measured, and the DNA content was calculated with a standard curve ($R^2 = 0.999$) prepared using a calf-thymus DNA (Sigma Aldrich, USA).

2.10 Alkaline phosphatase assay

The osteoblastic differentiation was evaluated by the alkaline phosphatase (ALP) activity assay using *p*-nitrophenol phosphate (pNPP) as a substrate. The cell lysates at 7, 14 and 21 days of the culture were prepared as the same as the DNA quantification. Fifty microliter of the lysate was mixed with 50 μL of pNPP in the 96-well microplate and incubated at 37 °C for 30 min. The reaction was stopped by adding 1 N NaOH and the amount of *p*-nitrophenol (pNP) was calculated from a light absorbance at 405 nm using a standard curve prepared from serial dilutions of pNP. The measurement was repeated five times in each sample. The ALP amount was normalized against the amount of the total DNA amount in each sample.

2.11 Statistical analysis

All data were expressed as mean ± standard deviation (SD). Student *t*-test and one-way analysis of variance performed to reveal significant differences. Turkey's post hoc test was performed for pairwise comparison with a level of significance, *p*, at less than 0.05.

3 Results

3.1 Hydrothermally converted sea urchin tests

Figure 1 shows naked-eye observations of sea urchin skeletons before and after hydrothermal phosphatization. The macroscopic shape was retained and its color was removed after treatment. Scanning electron microscopic images of the SU2, shown in Fig. 2a and b, revealed that the skeleton had a highly porous and interconnected microstructure composed of macropores in the range of 200–300 μm and micropores in the range of 20–50 μm. Magnesium was

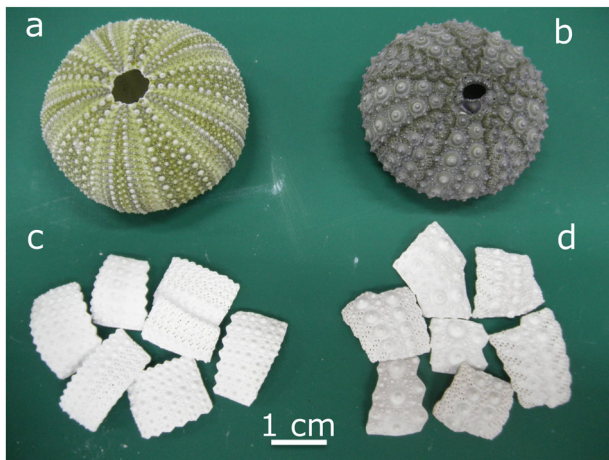
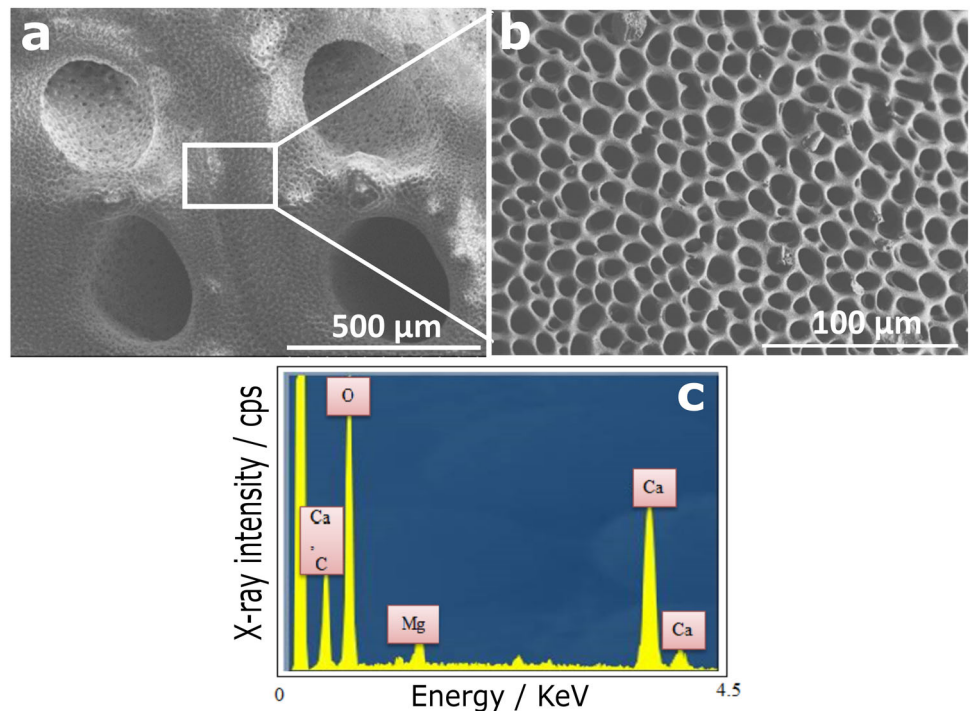


Fig. 1 Naked eye view of a SU1, b SU2, c CP1 and d CP2

Fig. 2 SEM images of SU2 a–b and c shows the EDS pattern of sample surface



detected in the SU2 by the EDS is shown in Fig. 2c. Those of the SU1 showed the similar results.

Figure 3 shows the XRD results of the SU2, CP2 and CPC2. The SU2 was identified as calcite (JCPDS 5-586) single phase; thus, the SU2 was Mg-containing calcite as stated in previous reports [29, 33]. The CP2 was composed

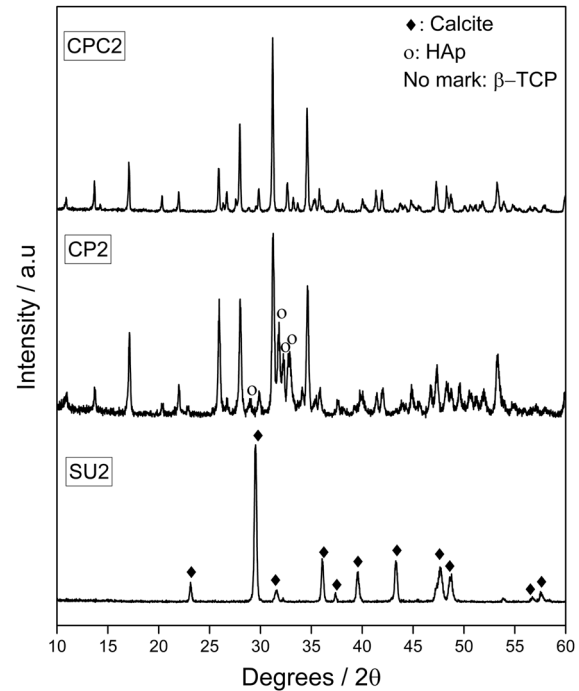


Fig. 3 XRD pattern of SU2, CP2 and CPC2

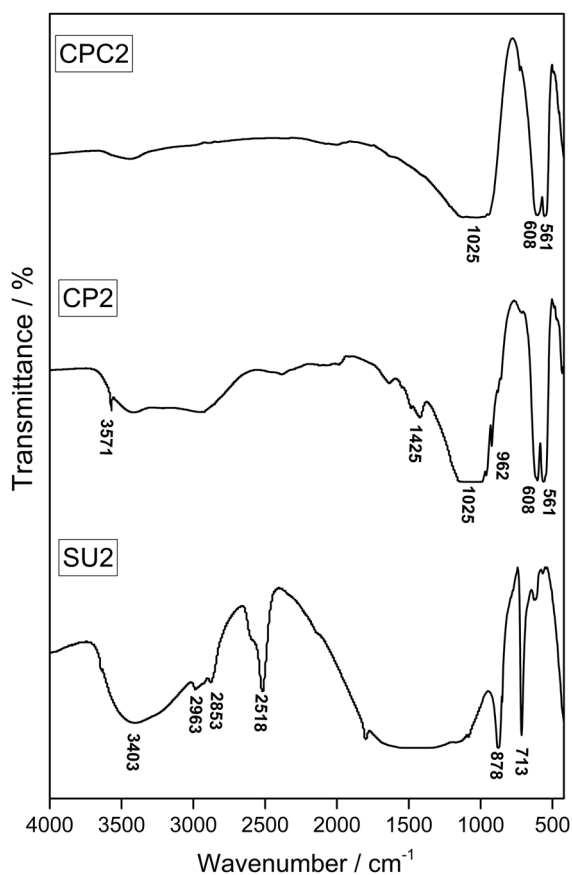


Fig. 4 FTIR spectra of SU2, CP2 and CPC2

of two phases, β -tricalcium phosphate (β -TCP, JCPDS 9–619) and hydroxyapatite (HAp, JCPDS 9–432). After the hydrothermal phosphatization, the SU2 transformed to a biphasic calcium phosphate (BCP) consisting of Mg-containing β -tricalcium phosphate and a small amount of hydroxyapatite. From the XRD pattern of CPC2, HAp phase was disappeared and became a β -TCP single phase. The SU1, CP1 and CPC1 demonstrated the similar results in the XRD data to the SU2, CP2 and CPC2, respectively. The amount of β -TCP and HAp formed in CP1 and CP2 calculated from XRD pattern is shown in Table 1.

The FT-IR results of the SU2, CP2 and CPC2 are shown in Fig. 4. Internal modes of carbonate in calcite at 713, 878 cm^{-1} and broad absorption band around 1450 cm^{-1} was detected in the SU2. The CP2 spectrum showed absorption bands for PO_4^{3-} bending mode at 608 and 561 cm^{-1} ; stretching mode at 962 and 1025 cm^{-1} ; absorption bands for CO_3^{2-} anti-symmetric stretching mode at 1425 cm^{-1} and OH^- stretching mode at 3571 cm^{-1} , but no absorption bands from organic substances were detected. The spectrum of the CPC2 showed no differences with that of the CP2 except for an absence of the CO_3^{2-} and OH^- absorption band. Overall assignments are given in Table 2 [34]. As the same as the XRD results, the FT-IR data for the SU1, CP1

Table 1 Quantitative analysis from XRD

Sample	β -TCP (%)	HAp (%)	Ca/P
CP1	82.5	17.5	1.53
CP2	82.0	18.0	1.53

Table 2 Band assignments of FTIR spectrum given in Fig. 4

Wavenumber (cm^{-1})	Assignment/s
3571	O-H stretching from hydroxyapatite
2963, 2853, 2518	Organic constituents (bio-polymer)
1425	CO_3^{2-} anti-symmetric stretching
1025	P-O in HPO_4 and PO_4 groups (stretching mode)
962	P-O in PO_4 group
878	CO_3^{2-} out of plane bending
713	CO_3^{2-} anti-symmetric bending
608, 561	P-O in PO_4 groups (bending mode)

and CPC1 showed the similar results to SU2, CP2 and CPC2, respectively.

Scanning electron microscopic images of the CP2 and related EDS spectrum are shown in Fig. 5. Figure 5a and b show SEM image of low and high magnification image of the CP2, where the diameter of the pores ranged from 200 to 250 μm and 20 to 40 μm , respectively. These images demonstrated that the CP2 still retains the porous microstructure of the original skeleton. The EDS spectrum (Fig. 5c) indicates the characteristic peaks of calcium, magnesium, phosphorous and oxygen, which demonstrates that Mg was retained after hydrothermal phosphatization. The similar results were obtained for the CP1 observations.

Quantitative chemical analyses and (Ca + Mg)/P atomic ratios from the ICP-AES data, as shown in Table 3, revealed no significant differences in the (Ca + Mg)/P ratio between CP1 and CPC1; and CP2 and CPC2.

3.2 Characterization of the scaffolds

The naked eye observation of the scaffolds, CPC1 and CPC2, is shown in Fig. 6a. The scaffolds can be fabricated into any shape and hence they are shape controllable. The microstructures of the horizontal cross sections of the scaffolds are shown in Fig. 6b–f. The scaffolds had an open pore microstructure with a high degree of interconnectivity and the microstructure of the CP1/CP2 granules was well maintained.

The open porosities and bending strengths at dry condition of the scaffolds are shown in Table 4. Most of the pores were still accessible and contributed to the total open porosity. The bending strengths of the scaffolds under wet

Fig. 5 SEM images of CP2 **a–b**. **c** Shows the EDS pattern of sample surface

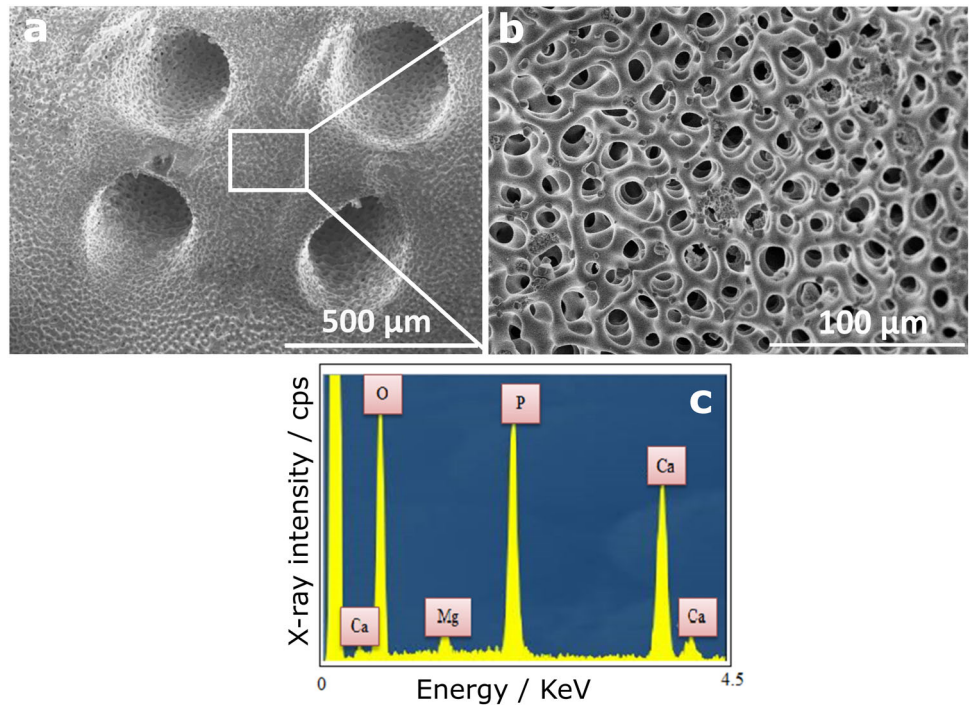


Table 3 Quantitative analysis from ICP-AES

Sample	Mg/Ca	(Ca+Mg)/P
SU1	0.1179 ± 0.0006	–
CP1	0.1196 ± 0.0002	1.5207 ± 0.0223
CPC1	–	1.5050 ± 0.0211
SU2	0.1205 ± 0.0001	–
CP2	0.1226 ± 0.0006	1.5217 ± 0.0153
CPC2	–	1.5097 ± 0.0090

condition could not be measured because the scaffolds became too soft for measurement. Even the scaffolds became soft; they can be easily handled by hand and forceps.

From stability analysis, where the scaffolds were soaked in PBS, 37 °C showed that they were able to maintain their shapes. The collagen used as a binder in the present study, was not decomposed to gelatin at 37 °C and maintained the integrity of the scaffold.

3.3 Biocompatibility

MG-63 cells seeded on the scaffolds attached to the surface and continue to grow in vitro. The cells demonstrated good initial attachment to the surfaces of scaffolds after day 1 of cell seeding as shown in Fig. 7a and b. According to the SEM observations at day 7, cells showed good migration

and proliferation into the pores of CP1/CP2 granules (Fig. 7c and d)

The live/dead staining images of the cells over the scaffolds after day 1 and 7 days of culture are shown in Fig. 8. The results showed that most of the cells were viable and very few or negligible dead cells were found in both the scaffolds.

Cell proliferations, evaluated by time-dependent changes of DNA amounts in the cell/scaffold constructs, indicated that the MG-63 cells in the scaffolds (Fig. 9) demonstrated significantly higher proliferation than that of the control, conventional collagen sponges, at day 7, 14 and 21.

The ALP activity shown in Fig. 10 revealed that significantly high ALP activities were observed at day 14 and 21 for the test group in comparison to the control collagen sponge group, though no significant differences on day 7. This suggested that the presence of BCP granules stimulated an early stage of osteoblastic differentiation.

4 Discussion

4.1 Phosphatization

The sea urchin skeletons used in this study are waste products of sea urchin food processing industry in Japan. From SEM imaging, it is revealed that the skeletons are made up of highly interconnected porous structure with both macropores and micropores. X-ray diffraction analysis revealed that the composition of skeletons is Mg-calcite and EDS

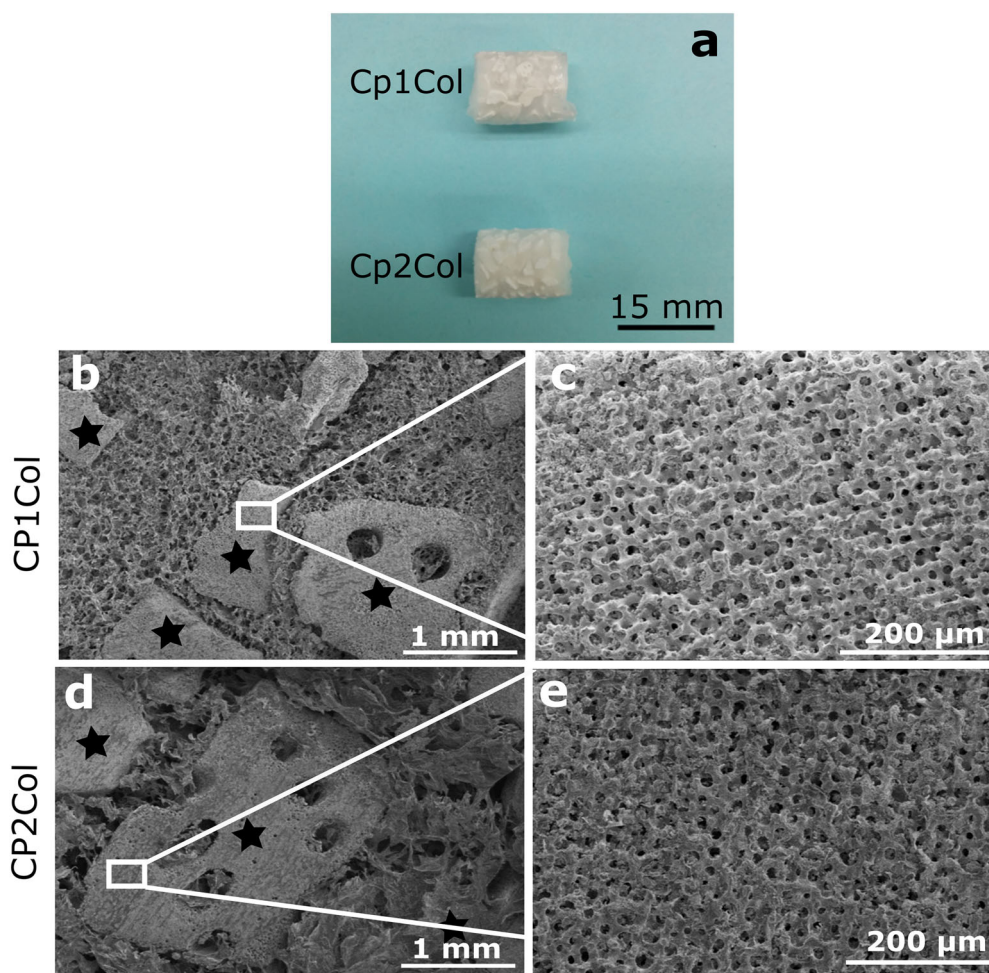


Fig. 6 **a** Naked eye view of the scaffolds. SEM images of horizontal cross section of CP1Col **b–c** and CP2Col **d–e** scaffolds. Closed stars in image **b,d** indicates CPI and CP2 granules respectively

Table 4 Open porosity and bending strength of scaffolds

Scaffold	Open porosity (%)	Bending strength (dry state, kPa)
CP1Col	81.94 ± 1.34	159.89 ± 31.39
CP2Col	83.84 ± 2.38	149.71 ± 27.35

analysis showed no contamination from heavy metal ions. The SEM analysis of CPI/CP2 showed that the converted skeletons retained their original porous structure.

From XRD and FTIR analysis, hydrothermal phosphatization of sea urchin skeleton converted Mg-calcite to BCP consisting mainly of Mg-containing β -TCP (82%) and a small amount of HAp (18%). Hydrothermal conversion of other marine CaCO_3 skeletons, such as coral, cuttlebone and sea shells, has been reported to produce HAp, while sea urchin spines produced β -TCMP [35]. The phosphatization reaction could be a dissolution-re-precipitation process [36] of Mg-calcite and calcium phosphate; where, all re-precipitation process of calcium phosphate occurred on

the surface of Mg-calcite and progressed towards the Mg-calcite side, with the dissolution of Mg-calcite. In addition, from the viewpoint of density, TCP and HAp crystals have densities of 3.14 and 3.16, respectively; thus, cavity formed by dissolution of Mg-calcite, density could be less than that of calcite, 2.71, this would provide enough space for TCP and/or HAp formation towards Mg-calcite instead of outside of sea urchin skeleton.

Generally, calcite phosphatization at high-temperature results formation of calcium-deficient and carbonate-containing hydroxyapatite crystals [14]. The formation of β -TCP instead of HAp in the present study is explained by the presence of Mg^{2+} ions, well-known as an inhibitor of HAp formation and stabilizer of the β -TCP structure [37]. In addition, Mg^{2+} ions in calcite structure may additionally be unstable than Ca^{2+} ions, because Mg^{2+} ions do not supersede calcite crystals more than 10% in the atomic ratio for Ca^{2+} even if the solution consists of high Mg^{2+} concentration [38], and may preferably release from Mg-calcite in comparison to Ca^{2+} ions. Therefore, the Mg/Ca atomic

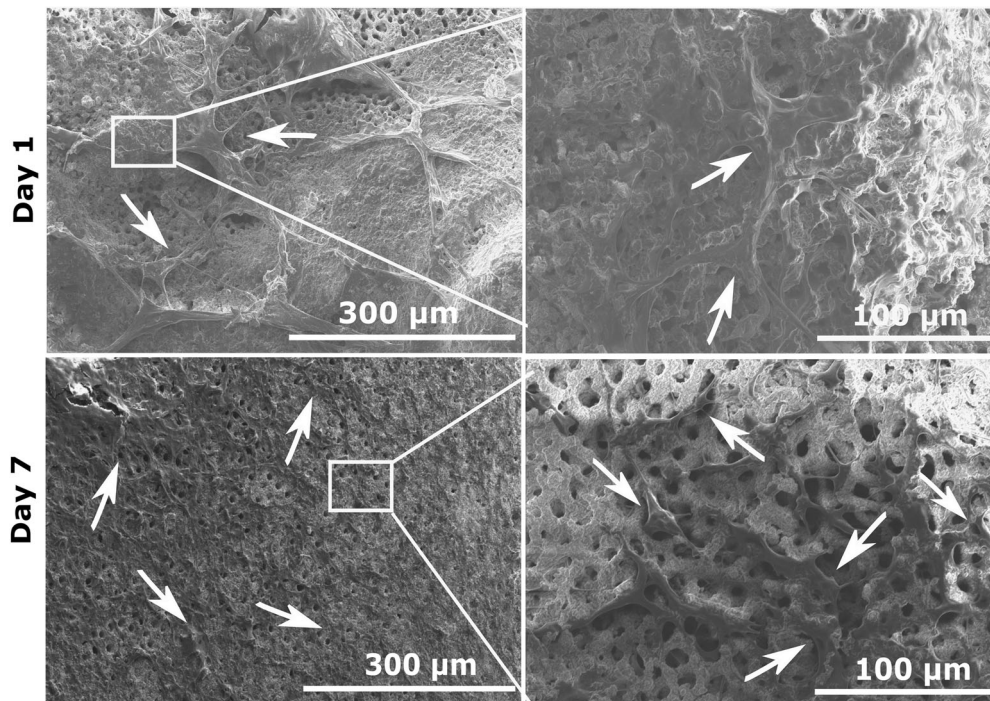


Fig. 7 Vertical cross section SEM images of MG-63 cells cultured on CP2Col scaffold after day 1 **a–b** and day 7 **c–d**. White arrows indicate the regions of adhered cells

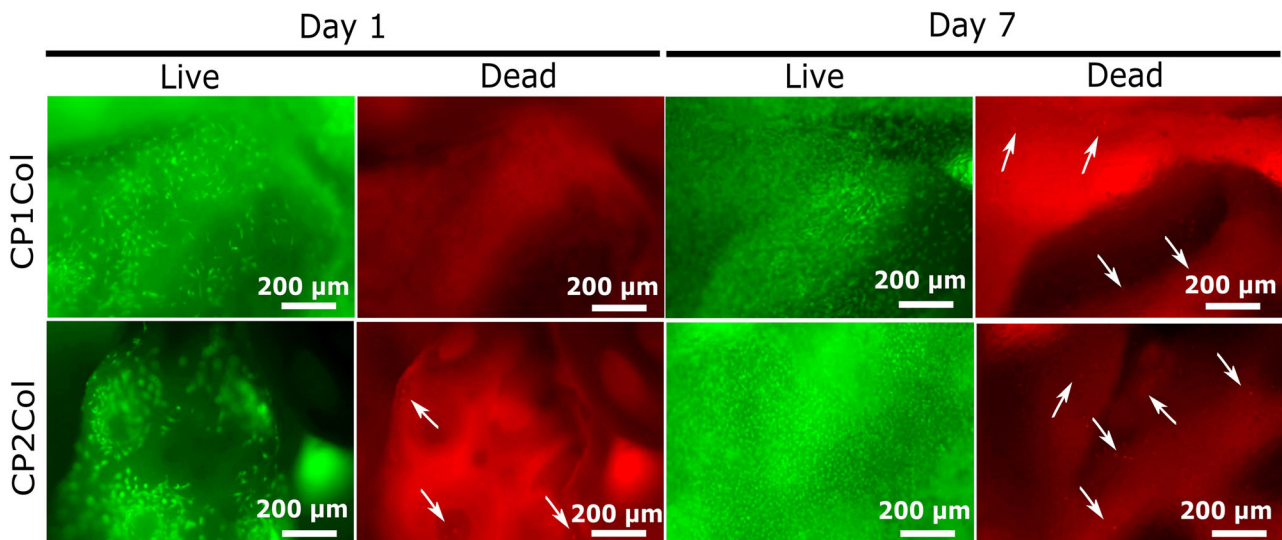


Fig. 8 Viability fluorescence images of scaffolds. Calcein acetoxyethyl (Calcein AM) stained healthy cells appeared as green, and propidium iodide stained nuclei of dead cells appeared as red. White arrows indicate the dead cells

ratio in the solution at an early stage of phosphatization could be higher than that in sea urchin skeletons and these Mg^{2+} ions stabilize as well as incorporate into β -TCP. In the later stage, Mg^{2+} ion concentration could decrease to allow the formation of Ca-deficient HAp; thus, a small amount of HAp existed in the CP1 and CP2.

Further, the presence of large amounts of carbonate ions results in the formation of carbonate containing HAp, as

shown in FT-IR spectrum of CP2 (Fig. 4), also supported in the literature [14]. In addition, the carbonate-containing HAp obtained from the phosphatization was a Ca-deficient HAp as reported, because it gets easily decomposed to β -TCP at high temperature [39] which is confirmed by the XRD pattern (Fig. 3) and the FT-IR (Fig. 4) spectrum of the CPC2, respectively. Slightly high values of the theoretical Ca/P atomic ratios (Table 1) in comparison to the observed

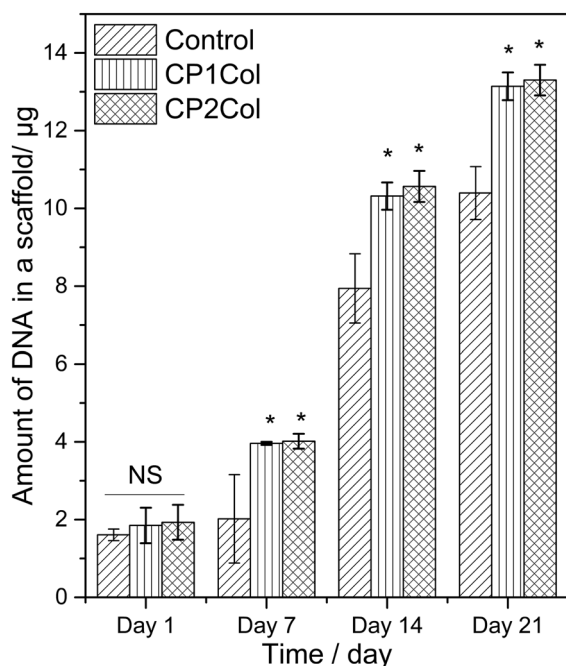


Fig. 9 Total DNA content assay of MG-63 cells cultured on scaffolds. Data are represented as mean \pm SD for 5 samples. *Indicates significant differences ($p < 0.05$) when compared with control. NS means no significant difference

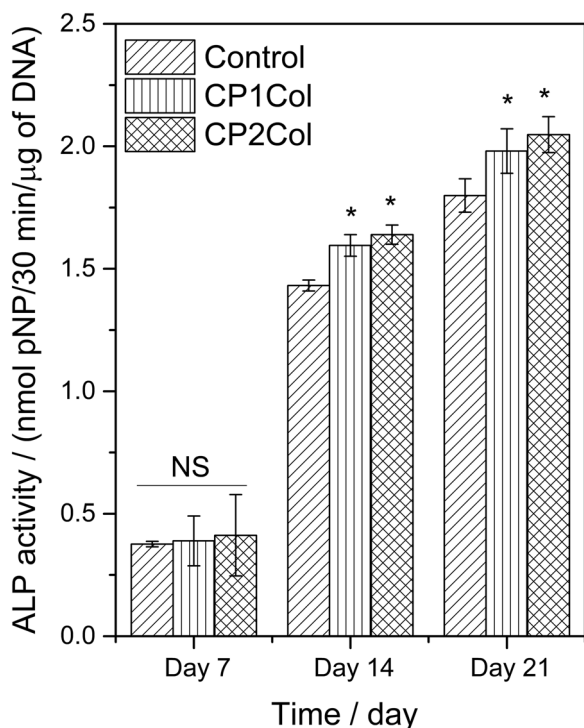


Fig. 10 Alkaline phosphatase activity assay of MG-63 cells cultured on scaffolds. Data are represented as mean \pm SD for 5 samples. *Indicates significant difference ($p < 0.05$) when compared control. NS means no significant difference

ratios (Table 3) also supported Ca deficiency of the HAp. No significant differences in observed atomic ratios of Ca, Mg and P between CPs and CPCs, which is very reasonable because they do not get vaporized at 1000 °C.

4.2 Scaffold properties

The scaffolds fabricated with collagen and the CP1 or CP2 granules showed good open porosity with both macropores and micropores, even after some pores were covered with the collagen fibers. This highly porous structure can be appropriate for the BTE applications to allow cell migration, vascularization and nutrient supplementation [40]. The scaffold was highly elastic in wet condition and could be molded into any shape to fit irregular bone defects. Overall, collagen acted as a binder and maintained the integrity of the scaffold due to the stability of collagen gel at 37 °C in the physiological ion conditions, while highly porous CP1 or CP2 granules reserved the space for bone formation.

Generally, bone tissue scaffolds fabricated from ceramics and/or polymers do not have sufficient mechanical strength for load bearing; however, the scaffolds have high capability to introduce bone tissues by appropriate time period, they would be useful for bone defect repairment. For instance, hydroxyapatite/collagen (HAp/Col) bone like nanocomposite sponge developed by Kikuchi et al. [41], demonstrated good clinical trial results [42] because of their sponge-like elasticity to fit any shape of bone defect, where no gaps remain between the host bone and scaffold. Gaps between the host bone and scaffold would generally delay the bone ingrowth process significantly. Similarly, the CP1Col/CP2Col composite in the present study, possess adequate mechanical strength under wet conditions and shape controllability to be used a bone substitute.

4.3 Biocompatibility of scaffolds

No significant cytotoxicity was observed in any scaffold. From mid vertical cross section images of SEM, cell adherence onto the granules and migration into their macropores were clearly observed. In addition, cell proliferation was highly enhanced in both the CP1Col and CP2Col scaffolds after day 7, 14 and day 21 in comparison to the control collagen sponge. The ALP activity at day 7 showed no significant differences among all the groups, due to the formation of cell-cell interactions in its peripheral area [43]. The increase in the ALP activity for the cells in the present scaffolds was higher and showed significant difference with that of the control collagen sponge, because calcium phosphate granules in the presently fabricated scaffolds could enhance the early stage of osteoblastic differentiation. Matsuno et al. [44], reported collagen disadvantages as a bone void filler, that the collagen sponge after implantation

degraded completely in 4 weeks, although the collagen sponge was replaced by soft connective tissue and newly formed bone without showing the formation of the typical bone network. In fact, collagen is phagocytosed by macrophages instead of osteoclasts; thus, no signal transduction to osteoblasts occurs and no bone formation is promoted.

Biphasic calcium phosphate possesses several advantages over HAp and TCP due to their controlled bioactivity and balance between resorption/solubilization which guarantees the stability of the biomaterial while promoting bone ingrowth [45]. A report by Eun-Ung Lee et al. [46], showed that BCP composite with collagen (BCPC) provided proper space maintaining capacity and osteoconductive property compared to collagen sponge and BCP block. This result suggests that BCPC can be efficiently utilized in various clinical applications.

In this study, highly porous sea urchin skeletons are converted to BCP granules without any change in the microstructure, by a relatively low cost and simple hydrothermal phosphatization method. The scaffolds fabricated with porous biphasic CP1/CP2 granules and collagen provided essential porosity, bioactive surface for cell attachment and proliferation. Also, the scaffolds created a favorable environment for differentiation of cells, which can favor increased bone formation in comparison with a collagen sponge. The scaffolds proved to be biocompatible and have the potential to be utilized as artificial bone filler.

5 Conclusion

Raw sea urchin skeleton was hydrothermally converted to biphasic calcium phosphate with 82% β -TCP and 18 % HAp, retaining their native porous structure. Collagen molecules acted as a binder and maintained the integrity of the scaffold. The scaffold showed good open porosity and adequate mechanical strength. Furthermore, the in vitro biological evaluation showed that the scaffolds were non-cytotoxic. The MG-63 cells adhered and distributed well in the scaffolds. The cell proliferation ability and ALP activity were higher in the scaffolds in comparison to the collagen sponge. These results suggest that scaffolds fabricated with calcium phosphate granules converted from sea urchin test and collagen could be a potential candidate for artificial bone filler.

Acknowledgements The authors would like to thank Mr. Taira Sato for his help with the ICP-AES analysis. The authors express their sincere thanks to Prof. Yagi Hiroki, Otaru University of commerce, Japan and Higashi-shakotan fishery cooperative for providing sea urchin tests. This study in part was supported by revitalizing a local community by the development of new materials with sea urchin shells, the program for a proportion of practical uses with fish industries waste resources, Shakotan, Hokkaido, Japan.

Compliance with ethical standards

Conflict of interest The authors declare that they have no competing interests.

References

1. Boskey AL, Coleman R. Aging and bone. *J Dent Res United States*. 2010;89:1333–48.
2. Young MF. Bone matrix proteins: their function, regulation, and relationship to osteoporosis. *Osteoporos Int Engl*. 2003;14 Suppl 3:S35–42.
3. Laurencin C, Khan Y, El-Amin SF. Bone graft substitutes. *Expert Rev Med Devices Engl*. 2006;3:49–57.
4. Finkemeier CG. Bone-grafting and bone-graft substitutes. *J Bone Jt Surg Am*. 2002;84–A:454–64.
5. Amini AR, Laurencin CT, Nukavarapu SP. Bone tissue engineering: recent advances and challenges. *Crit Rev Biomed Eng*. 2012;40:2.
6. Laurencin CT, Ambrosio AMA, Borden MD, Cooper JA. Tissue engineering: orthopedic applications. *Annu Rev Biomed Eng Annu Rev*. 1999;1:19–46.
7. Fröhlich M, Grayson W, Wan L, Marolt D, Drobnic M, Vunjak-Novakovic G. Tissue Engineered Bone Grafts: Biological Requirements, Tissue Culture and Clinical Relevance. *Curr. Stem Cell Res. Ther*. 2008;3(4):254–264.
8. Place ES, Evans ND, Stevens MM. Complexity in biomaterials for tissue engineering. *Nat Mater*. 2009;8:457–70.
9. Karageorgiou V, Kaplan D. Porosity of 3D biomaterial scaffolds and osteogenesis. *Biomaterials*. 2005;26:5474–91.
10. Oonishi H, Hench LL, Wilson J, Sugihara F, Tsuji E, Kushitani S, et al. Comparative bone growth behavior in granules of bio-ceramic materials of various sizes. *J Biomed Mater Res*. 1999;44:31–43.
11. Dhandayuthapani B, Yoshida Y, Maekawa T, Kumar DS. Polymeric scaffolds in tissue engineering application: A review. *Int J Polym Sci*. 2011; <https://doi.org/10.1155/2011/290602>.
12. LeGeros RZ. Properties of osteoconductive biomaterials: calcium phosphates. *Clin Orthop Relat Res*. 2002;395:81–98.
13. Yuan H, Yang Z, Li Y, Zhang X, De Bruijn JD, De Groot K. Osteoinduction by calcium phosphate biomaterials. *J Mater Sci Mater Med*. 1998;9:723–6.
14. Roy DM, Linnehan SK. Hydroxyapatite formed from coral skeletal carbonate by hydrothermal exchange. *Nature*. 1974;247:220–2.
15. Ben-Nissan B. Natural bioceramics: from coral to bone and beyond. *Curr Opin Solid State Mater Sci*. 2003;7:283–8.
16. Barros AA, Aroso IM, Silva TH, Mano JF, Duarte AR, Reis RL. In vitro bioactivity studies of ceramic structures isolated from marine sponges. *Biomed Mater*. 2016;11:45004.
17. Ivankovic H, Gallego Ferrer G, Tkalcec E, Orlic S, Ivankovic M. Preparation of highly porous hydroxyapatite from cuttlefish bone. *J Mater Sci Mater Med*. 2009;20:1039–46.
18. Vecchio KS, Zhang X, Massie JB, Wang M, Kim CW. Conversion of sea urchin spines to Mg-substituted tricalcium phosphate for bone implants. *Acta Biomater Engl*. 2007;3:785–93.
19. Clarke SA, Walsh P. Marine organisms for bone repair and regeneration. In: Mallick K, editor. *Bone Substituted Biomaterials*. 2014. p. 294–318.
20. Holzapfel BM, Reichert JC, Schantz J-T, Gbureck U, Rackwitz L, Nöth U, et al. How smart do biomaterials need to be? A translational science and clinical point of view. *Adv Drug Deliv Rev*. 2013;65:581–603.

21. Fellah BH, Gauthier O, Weiss P, Chappard D, Layrolle P. Osteogenicity of biphasic calcium phosphate ceramics and bone autograft in a goat model. *Biomaterials*. 2008;29:1177–88.
22. Bohner M. Silicon-substituted calcium phosphates—a critical view. *Biomaterials*. 2009;30:6403–6.
23. Habibovic P, Barralet JE. Bioinorganics and biomaterials: bone repair. *Acta Biomater Engl*. 2011;7:3013–26.
24. Kannan S, Rocha JHG, Agathopoulos S, Ferreira JMF. Fluorine-substituted hydroxyapatite scaffolds hydrothermally grown from aragonitic cuttlefish bones. *Acta Biomater*. 2007;3:243–9.
25. Holmes RE, Bucholz RW, Mooney V. Porous hydroxyapatite as a bone-graft substitute in metaphyseal defects. A histometric study. *J Bone Jt Surg Am*. 1986;68:904–11.
26. Vuola J, Taurio R, Goransson H, Asko-Seljavaara S. Compressive strength of calcium carbonate and hydroxyapatite implants after bone-marrow-induced osteogenesis. *Biomaterials*. 1998;19:223–7.
27. Das S, Mangwani N. Ocean acidification and marine microorganisms: responses and consequences. *Oceanologia*. 2015;57:349–61.
28. Akino M, Aso S, Kimura M. Effectiveness of biological filter media derived from sea urchin skeletons. *Fish Sci*. 2015;81:923–7.
29. Tamasan M, Ozyegin LS, Oktar FN, Simon V. Characterization of calcium phosphate powders originating from *Phyllacanthus imperialis* and *Trochidae Infundibulum concavus* marine shells. *Mater Sci Eng C*. 2013;33:2569–77.
30. Ağaoğullari D, Kel D, Gökçe H, Duman I, Öveçoğlu ML. Bio-ceramic Production from Sea Urchins. *Acta Physica Polonica A*. 2012;121:1–4.
31. Borzęcka-Prokop B, Weselucha-Birczyńska A, Koszowska E. MicroRaman, PXRD, EDS and microscopic investigation of magnesium calcite biomineral phases. The case of sea urchin biominerals. *J Mol Struct*. 2007;828:80–90.
32. Chang SJ, Huang Y-T, Yang S-C, Kuo S-M, Lee M-W. In vitro properties of gellan gum sponge as the dental filling to maintain alveolar space. *Carbohydr Polym*. 2012;88:684–9.
33. Tshipursky SJ, Buseck PR. Structure of magnesian calcite from sea urchins. *Am Mineral*. 1993;78:775–81.
34. Nyquist RA, Kagel RO. PREFACE BT—Handbook of infrared and Raman spectra of inorganic compounds and organic salts. San Diego: Academic Press; 1971. p. vii.
35. Zhang X, Vecchio KS. Conversion of natural marine skeletons as scaffolds for bone tissue engineering. *Front Mater Sci*. 2013;7:103–17.
36. Ishikawa K. Bone substitute fabrication based on dissolution-precipitation reactions. *Materials*. 2010;3:1138–55.
37. Kannan S, Ventura JM, Ferreira JMF. Aqueous precipitation method for the formation of Mg-stabilized β -tricalcium phosphate: an X-ray diffraction study. *Ceram Int*. 2007;33:637–41.
38. Reddy MM, Nancollas GH. The crystallization of calcium carbonate. *J Cryst Growth*. 1976;35:33–8.
39. Safronova TV, Putlyaev VI, Avramenko OA, Shekhirev MA, Veresov AG. Ca-deficient hydroxyapatite powder for producing tricalcium phosphate based ceramics. *Glas Ceram*. 2011;68:28–32.
40. Loh QL, Choong C. Three-dimensional scaffolds for tissue engineering applications: role of porosity and pore size. *Tissue Eng Part B*. 2013;19:485–502.
41. Kikuchi M, Koyama Y, Edamura K, Irie A. Synthesis of hydroxyapatite/collagen bone-like nanocomposite and its biological reactions. *Adv Nanocomposites—Synth Charact Ind Appl*. 2007;2:181–94.
42. Sotome S, Ae K, Okawa A, Ishizuki M, Morioka H, Matsumoto S, et al. Efficacy and safety of porous hydroxyapatite/type 1 collagen composite implantation for bone regeneration: a randomized controlled study. *J Orthop Sci*. 2016;21:373–80.
43. Yoshida T, Kikuchi M, Koyama Y, Takakuda K. Osteogenic activity of MG63 cells on bone-like hydroxyapatite/collagen nanocomposite sponges. *J Mater Sci Mater Med*. 2010;21:1263–72.
44. Matsuno T, Nakamura T, Kuremoto K, Notazawa S, Nakahara T, Hashimoto Y, et al. Development of beta-tricalcium phosphate/collagen sponge composite for bone regeneration. *Dent Mater J Jpn*. 2006;25:138–44.
45. Lobo SE, Livingston Arinze T. Biphasic Calcium Phosphate Ceramics for Bone Regeneration and Tissue Engineering Applications. *Mater*. 2010;3:815–826.
46. Lee E-U, Kim D-J, Lim H-C, Lee J-S, Jung U-W, Choi S-H. Comparative evaluation of biphasic calcium phosphate and biphasic calcium phosphate collagen composite on osteoconductive potency in rabbit calvarial defect. *Biomater Res*. 2015;19:1–7.